

# EARTH RADIATION PRESSURE EFFECTS ON SATELLITES

88-4292-CP

P. C. Knocke \*, J. C. Ries, and B. D. Tapley  
Center for Space Research  
The University of Texas at Austin, Austin, Texas

## Abstract

A diffuse earth radiation force model is presented, which includes a latitudinally varying representation of the shortwave and longwave radiation of the terrestrial sphere. Applications to various earth satellites indicate that this force, in particular the shortwave component, can materially affect the recovery of estimated parameters. Earth radiation pressure cannot explain the anomalous deceleration of LAGEOS, but can produce significant along track accelerations on satellites with highly eccentric orbits. Analyses of GEOS-1 tracking data confirm this result.

## Nomenclature

$a$	= albedo
$a_s$	= fraction of incident flux reflected by the satellite
$\ddot{a}$	= acceleration
$A'$	= projected attenuated area of earth element $dA$
$A_c$	= cross sectional area of satellite
$b_s$	= fraction of incident flux reemitted by the satellite
$c$	= speed of light
$C_D$	= drag coefficient
$dA$	= area of earth element
$e$	= emissivity (dimensionless)
$E_s$	= solar irradiance (Watts $m^{-2}$ )
$h$	= altitude (km.)
$j$	= subscript referring to the $j$ th earth element
$JD$	= Julian date of interest
$L$	= radiance (Watts $m^{-2}$ steradian $^{-1}$ )
$M$	= exitance (Watts $m^{-2}$ )
$P_n$	= $n$ th degree Legendre polynomial
$r$	= distance from earth element to satellite
$\hat{r}$	= unit vector pointing from earth element to satellite
$r_{EARTH}$	= earth-sun distance
$R$	= reflection law effectiveness coefficient
$R_E$	= radius of the earth
$\alpha$	= view angle (Fig. 2)
$\eta_R$	= solar radiation satellite reflectivity
$\eta_E$	= earth radiation satellite reflectivity
$\theta_s$	= solar zenith angle
$\xi$	= emission law effectiveness coefficient
$\phi$	= equatorial latitude
$\Phi$	= radiant flux (Watts)
$\psi$	= azimuth angle (Fig. 2)
$\omega$	= frequency of periodic earth radiation coefficients
$\Omega$	= solid angle (steradians)

## Introduction

Analyses of very accurate laser ranging observations

\*Research Engineer Scientist Assistant Student Member, AIAA

indicate that the semimajor axis of the geodetic earth satellite LAGEOS undergoes an unexplained mean secular decrease of approximately 1.1 mm/day, once all known force effects are taken into account.<sup>11</sup> Large and complex periodic variations of the semimajor axis about this mean secular decrease are observed as well. Various force effects, including earth radiation pressure, have been proposed to explain the drag-like phenomenon behind this anomalous behavior. As part of an ongoing effort to understand the responsible mechanism or mechanisms driving this effect, an earth radiation pressure model has been developed for the University of Texas Orbit determination program (UTOPIA). A rigorous investigation of this force is desirable from the perspective of improving force models and avoiding inaccuracies in some estimated parameters. The following treatment describes the underlying radiation mechanics, assumptions, and computational characteristics of the model, as well as the orbital effects suggested by its application, and its impact on the estimation of orbit and force model parameters. Although the LAGEOS anomaly has provided the initial impetus for this study, an examination of the effects of earth radiation pressure on other satellites, especially those with highly eccentric orbits, furnishes fresh insights into the influence of this force.

The orbital influence on satellites of radiation pressure due to solar flux reflected and re-emitted from the earth has been examined for more than twenty years. Wyatt, Lautmann and others have analyzed the phenomenon using various assumptions (e.g. uniform albedo, no terminator) designed to simplify the surface integrals which arise from the mechanics of radiative transfer from an extended body like the earth.<sup>4,17</sup> Anselmo, et al. avoid the complications of this representation by means of a simple analytical model which furnishes transverse "kicks" as the satellite passes over the terminator.<sup>1</sup> Lochry solves the integral problem through a clever choice of coordinate systems, but the resulting expressions are not well disposed to either parameterization or flexibility in the representation of the albedo and longwave emissivity.<sup>5</sup> Rubincam and Weiss provide an elegant analytical integration of the shortwave earth radiation pressure equations through the use of a spherical harmonic representation of albedo.<sup>8</sup> The expressions in this case are extremely complicated and restricted primarily to low eccentricity satellites, a purely zonal albedo distribution, and diffuse radiation mechanics. McCarthy and Martin's earth radiation pressure calculation method has been chosen as the basis of the model for UTOPIA, because of its generality, simplicity, and flexibility.<sup>6</sup>

Wyatt, Lochry, and others have predicted that the magnitude of the earth radiation pressure should be approximately equal to 10% to 25% of the direct solar radiation pressure for most satellites.<sup>5, 17</sup> In fact, at very low altitudes (200 to 300 km.) the magnitude of earth radiation pressure can be 35% of the direct solar pressure. Measurements by accelerometers aboard drag make-up satellites like CACTUS tend to verify these estimates, and

provide empirical evidence for the physical existence and orbital influence of the earth radiation pressure.<sup>3</sup>

It has been suggested that the residual secular or periodic variations in the semimajor axis of LAGEOS may be driven by fluctuations in earth radiation pressure arising from diurnal variations in albedo or the anisotropic nature of reflected sunlight. Morgan attributes the deceleration to the effects of a morning-evening difference in albedo, coupled with specular reflection.<sup>7</sup> Barlier, et al. argue that anisotropic earth reflection creates an along-track acceleration with the same periodicities as the drag-like force, but of too small a magnitude.<sup>2</sup> Walch's analyses, based on CACTUS data, conclude that anisotropic reflection is too small to account for LAGEOS' drag-like force.<sup>15</sup> Rubincam, et al. use an extreme model, in which earth's northern hemisphere is assumed purely diffuse, and the southern hemisphere is assumed to reflect highly anisotropically, to argue that directional reflectance cannot explain the residual deceleration on LAGEOS.<sup>9</sup>

In a separate paper, Rubincam makes a persuasive case for attributing the greater portion of the secular decrease to a thermal inertia force pumped by infrared earth radiation.<sup>10</sup> This model does not explain the periodic variations in the drag-like force, however.

### Solar Radiation, Earth Radiation, and Albedo

When solar radiation hits the earth-atmosphere system, some percentage of this flux is immediately reflected and scattered as broadband shortwave radiation (i.e. radiant energy with wavelengths between approximately 0.2  $\mu\text{m}$  and 4.0  $\mu\text{m}$ ). The albedo of a surface is the ratio of the total broadband shortwave flux emanating from the element (in all directions) to the total broadband shortwave flux incident on the surface. It is clear that albedo is, first, not restricted to purely visible wavelengths, and second, is an integrated quantity.

Not all the incident solar energy is reflected. The balance is absorbed and re-emitted in delayed fashion as longwave infrared radiation above 4  $\mu\text{m}$  in wavelength. This is the "heat radiation" or emitted radiation of the earth, and is considered separately from the near-IR constituent of the reflected radiation.

### The Diffuse Earth Radiation Pressure Model

#### The Force Model

The calculation of the earth radiation pressure force on a satellite is based on the model by McCarthy and Martin, in which the portion of the earth's surface "visible" to the satellite is first divided into discrete segments, as shown in Figure 1. The incremental acceleration due to diffuse shortwave and longwave radiation from each segment is calculated using Lambert's law of diffuse radiation, assuming that each segment may be approximated as a plane surface tangent to the center of the segment. It is also assumed that the satellite may be approximated as a sphere with constant cross-sectional area. The incremental accelerations are summed vectorially to obtain the aggregate effect.

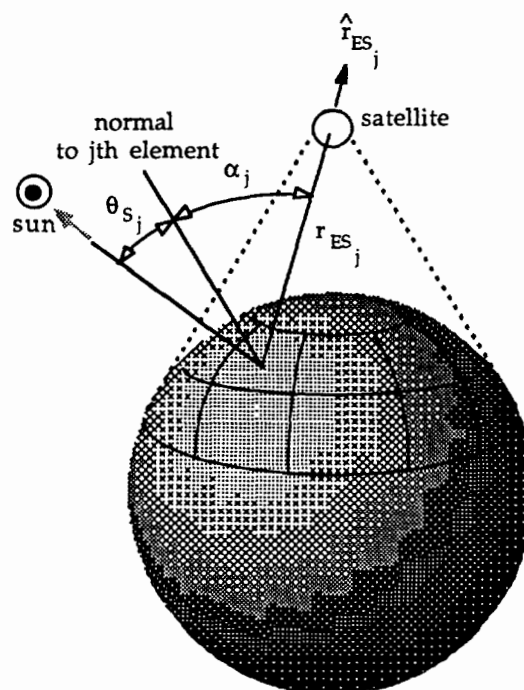


Fig. 1 Earth Radiation Pressure Model

#### Satellite-intercepted Flux in terms of Radiances

Consider the influence of a single earth element. In the following discussion, an earth "element" or "segment" refers to a reflecting/emitting surface with the same planetary albedo and longwave emissivity as the earth-atmosphere system at that point. This surface is assumed to be located at the surface of a spherical earth with radius equal to the mean radius of the true earth.

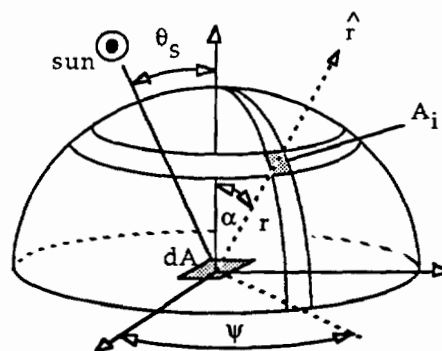


Fig. 2 Radiance Geometry

Suppose that a (planar) earth element of area  $dA$  has a certain radiance  $L$ , which may be due to reflected radiation or longwave radiation. Radiance is defined as follows:<sup>13</sup>

$$L = \frac{d\Phi}{d\Omega \, dA \, \cos \alpha} \quad (1)$$

where  $d\Phi$  = portion of the total flux radiated by earth element  $dA$  which is intercepted by  $A_i$ ,  
 $d\Omega$  = solid angle  $A_i/r^2$ ,  
 $r$  = distance from earth element  $dA$  to

intercepting element  $A_i$ ,  
 $A_i$  = area which intercepts the flux, normal to the  
 line from  $dA$  to  $A_i$ .

Thus, the flux intercepted by  $A_i$  is:

$$d\Phi = L \frac{A_i}{r^2} dA \cos \alpha. \quad (2)$$

In fact, it can be shown that any body presenting a cross sectional area  $A_c$  to the radiating element intercepts the following flux:

$$d\Phi = L \frac{A_c}{r^2} dA \cos \alpha. \quad (3)$$

Recall that radiance is a wavelength-dependent quantity, and that the earth radiates in two spectral bands, the shortwave and the longwave. Thus, to sufficient accuracy, the total satellite-intercepted flux due to a single earth element  $dA$  may be expressed as follows:

$$\begin{aligned} d\Phi_{TOT} &= d\Phi_{SW} + d\Phi_{LW} \\ d\Phi_{TOT} &= (L_{SW} + L_{LW}) \frac{A_c}{r^2} dA \cos \alpha \end{aligned} \quad (4)$$

where  $L_{SW}$  = total broadband shortwave radiance of  $dA$ ,

$L_{LW}$  = longwave radiance of  $dA$ .

#### Shortwave Radiance in terms of Albedo: Lambert's Law

The above expressions are fairly general representations of the satellite-intercepted radiation fluxes in terms of radiances. Consider now the shortwave flux, and its relation to classical albedo.

The albedo of element  $dA$  is defined as follows:

$$a = \frac{\Phi_{OUT_H}}{\Phi_{IN}}, \quad (5)$$

where  $\Phi_{OUT_H}$  = total shortwave flux out of  $dA$  intercepted by a hemisphere centered at  $dA$  and arcing above it. (See Figure 2.)

$\Phi_{IN}$  = total solar flux incident on  $dA$ .

Referring to Equation (2), the total hemispherical shortwave flux out of  $dA$  is:

$$\begin{aligned} \Phi_{OUT_H} &= \int_{hem.} L_{SW} dA \cos \alpha \frac{A_i}{r^2} \\ \Phi_{OUT_H} &= dA \int_{hem.} L_{SW} \cos \alpha \frac{r d\alpha r \sin \alpha d\psi}{r^2} \\ \Phi_{OUT_H} &= dA \int_{\psi=0}^{2\pi} \int_{\alpha=0}^{\frac{\pi}{2}} L_{SW} \sin \alpha \cos \alpha d\alpha d\psi \end{aligned} \quad (6)$$

where  $\int_{hem.}$  denotes integration over the hemisphere.

In order to proceed from this point, one must know how the radiance  $L_{SW}$  varies with the view angle  $\alpha$  and the

azimuth  $\psi$ . In general, this is a function of surface properties, but it is known that all reflecting surfaces exhibit characteristics situated between two extremes. One extreme is defined by specular (mirrorlike) reflection, where  $L_{SW}$  is strongly dependent on the orientation angles. At the other extremity is purely diffuse reflection, also known as isotropic reflection, in which the radiance is constant for all values of  $\alpha$  and  $\psi$ . Most surfaces exist somewhere between these limits, and must be described in terms of more complicated bidirectional reflectance laws.

Wyatt states that if one were to consider the earth-atmosphere system as a combination of purely specular components and purely diffuse components, the specular shortwave flux would amount to only 10% of the diffuse shortwave flux.<sup>17</sup> This makes intuitive sense, as the only sources of true specular reflection on the earth should be calm bodies of water such as lakes. Also, satellite radiance measurements reveal that all earth "surface" elements (e.g. snow, ice, cloud, and ocean) behave more or less diffusely at low solar zenith angles, and anisotropically only at higher solar zenith angles.<sup>14</sup> Because the illumination of an element varies as the cosine of the solar zenith angle, one might conclude that any portion of the earth-atmosphere system is likely to behave nearly diffusely during periods of high illumination, and become significantly anisotropic only during intervals of low illumination, when the earth radiation pressure is small in any event. All this lends weight to the argument that earth radiation pressure may be calculated to acceptable accuracy using a diffuse earth model. This conjecture requires validation, however, by more sophisticated analyses of anisotropy and its influence on earth radiation pressure.

On the strength of these arguments, it is assumed, in accordance with McCarthy and Martin, that shortwave earth radiation may be modeled as purely diffuse, to sufficient accuracy. The longwave component, which also is assumed to be purely diffuse, is dealt with in subsequent sections. Thus, the earth-atmosphere system qualifies as a Lambertian surface (purely diffuse reflector and emitter) and may be described via Lambert's law:

$$L(\alpha, \psi) = L, \text{ a constant.} \quad (7)$$

Equation (7) may now be integrated, as follows:

$$\begin{aligned} \Phi_{OUT_H} &= L_{SW} dA \int_{\psi=0}^{2\pi} \int_{\alpha=0}^{\frac{\pi}{2}} \sin \alpha \cos \alpha d\alpha d\psi \\ &= \pi L_{SW} dA \end{aligned} \quad (8)$$

Equation (8) defines the flux exiting  $dA$ . In order to relate albedo and shortwave radiance through Equations (5) and (8), the total solar flux incident on the surface must also be evaluated. The total amount of solar flux incident on a (planar) earth element is:

$$\Phi_{IN} = E_s \cos \theta_s dA \quad (9)$$

Both  $\theta_s$  and  $dA$  are illustrated in Figure 2.  $E_s$ , the "local" solar irradiance, is defined as the total radiant flux density of the sun at a point in space corresponding to the location of the earth at the time of interest. If the sun is assumed to be an isotropic source, the total solar flux is related to  $E_s$  as



follows:

$$E_s = \frac{\Phi_{\text{SUN}}}{4\pi R_{\text{EARTH}}^2} \quad (10)$$

where  $\Phi_{\text{SUN}}$  = total solar flux.

Combining Equations (5), (8), and (9) yields the following expression for the albedo of a diffusely reflecting surface in terms of its radiance:

$$a = \frac{\pi L_{\text{SW}}}{E_s \cos \theta_s}$$

Thus,

$$L_{\text{SW}} = \frac{a E_s \cos \theta_s}{\pi} \quad (11)$$

#### Longwave Radiance in terms of Emissivity

Emissivity is used to characterize the longwave infrared flux in the UTOPIA model of earth radiation pressure. The emissivity of an earth element  $dA$  is defined as follows:

$$e = \frac{M_{\text{LW}}}{M_B} \quad (12)$$

where  $M_{\text{LW}}$  = longwave exitance of  $dA$ ,

$M_B$  = exitance of  $dA$ , assuming the earth is an ideal black body (perfect absorber) which re-emits all the incident solar radiation isotropically.

Exitance is defined as follows:

$$M = \frac{\Phi}{dA}$$

Thus,

$$M_B = \frac{\text{earth-intercepted solar flux}}{\text{surface area of the earth}} = \frac{E_s \pi R_E^2}{4\pi R_E^2} = \frac{E_s}{4} \quad (13)$$

Now  $M_{\text{LW}}$  must be converted into radiance. Assuming  $dA$  is a diffuse emitter:

$$M_{\text{LW}} = \frac{\Phi_{\text{LW}}}{dA} = \frac{\int_{\psi=0}^{2\pi} \int_{\alpha=0}^{\pi/2} L_{\text{LW}} \sin \alpha \cos \alpha \, d\alpha \, d\psi}{dA}$$

$$M_{\text{LW}} = \pi L_{\text{LW}} \quad (14)$$

Thus,

$$L_{\text{LW}} = \frac{e M_B}{\pi} \quad (15)$$

As with the reflected flux, the emitted flux is assumed to be diffuse. For most bodies, and especially for the earth, this assumption is quite good. The nature of the earth-emitted

flux is that of "delayed" (and therefore nearly isotropic) thermal reradiation of the incident flux.

#### Earth Radiation Pressure Acceleration on a Spherical Satellite

Combining Equations (4), (11), and (15) yields the following expression for the total diffuse flux intercepted by a satellite with cross sectional area  $A_c$ , located at a distance  $r$  from a radiating element  $dA$  possessing albedo  $a$  and emissivity  $e$ :

$$d\Phi_{\text{TOT}} = (a E_s \cos \theta_s + e M_B) \frac{A_c}{\pi r^2} \cos \alpha \, dA \quad (16)$$

#### The Satellite Model:

##### Lochry's Radiation Augmentation Factor

The total force engendered by the satellite-intercepted radiant flux has three primary components. The first constituent is the "black body" force, i.e. the force which the body would experience if it were a perfect absorber. This force always points in the direction of the incident flux, regardless of the geometry of the intercepting body, or its reflective and emissive properties. The second component is the force arising from reflected flux. In general, this force is not directed along the line of incident flux. The third constituent of the total radiation pressure acceleration is that due to absorbed radiation thermally re-emitted from the satellite.

In the context of modeling the dynamic effect of these radiation phenomena, Lochry defines a useful "augmentation factor"  $K$ :

$$K = 1 + a_s R + b_s \xi \quad (17)$$

where the unity term refers to the "black body" force mentioned above.  $R$  and  $\xi$  are functions of the body's reflection and emission laws (e.g. specular or diffuse), geometry, and orientation.

The primary utility of the augmentation factor lies in describing the dynamical effect of radiation pressure on a sphere, a flat plate oriented normal to the flux, or any other configuration in which the resultant radiation pressure acceleration is along the line of incident flux. (For a given earth element, as illustrated in Figure 2, the line of incident flux is defined by the vector  $\hat{r}$ .) In this context, an "effectiveness coefficient" is a measure of the efficiency with which satellite-reflected or -emitted flux generates thrust along the element-satellite line. For example, a specularly reflecting flat plate normal to the incident flux has a reflection effectiveness measure of  $R = 1$ . This indicates that all of the reflected flux is bounced back towards the source. The emission law effectiveness coefficient is simpler to characterize. If the satellite reradiates energy "promptly", i.e. before the occurrence of substantive heat transfer, then the emissions are diffuse, with dynamical effects identical to those of diffusely reflected flux. If the intercepting body is a perfect conductor, then the emitted radiation is "delayed" isotropic reradiation. Because the body emanates equally in all directions, the net dynamic effect is zero, and  $\xi = 0$ . Thus:

$$0 \leq \xi \leq R_d,$$

where  $R_d$  is the reflection law effectiveness coefficient for a diffusely reflecting body configured such that the net radiation pressure is directed along the line of incident flux.

The range of  $K$  may be deduced from the above considerations, and by assuming, reasonably, that all the incident energy is either reflected or emitted (i.e.  $a_s + b_s = 1$ ). Thence:

$$1 \leq K \leq 2,$$

where unity refers to the case of total absorption, and  $K=2$  corresponds to the case of a flat, perfect reflector oriented normal to the incident flux ( $\alpha = 1$ ,  $R = 1$ ).

In sum, the acceleration experienced by a satellite of mass  $m$ , due to diffuse shortwave and longwave radiation emanating from a single earth element is:

$$d\vec{a} = K \frac{d\Phi_{TOT}}{mc} \hat{r} \quad (18)$$

or

$$d\vec{a} = K (a E_s \cos \theta_s + e M_B) \frac{A_c \cos \alpha dA}{mc \pi r^2} \hat{r}. \quad (19)$$

#### The Total Acceleration due to all Earth Elements

A rigorous evaluation of the total effect of earth radiation pressure requires the integration of Equation (19) over an "effective cap", whose apex is located at the subsatellite point and includes all points on the earth in direct line of sight to the satellite. Both Lochry and Rubincam and Weiss pursue analytical approaches to this problem, resulting in solutions which tend to be dependent on a particular albedo model, an inflexible assumption of diffusivity, or low eccentricity orbits.<sup>5, 8</sup> To avoid these difficulties, the integration is replaced with a simple summation over a small number of discrete earth elements.

Thus, the total acceleration on a spherical satellite of constant cross sectional area and invariant reflective and emissive properties, due to diffuse radiation from all "effective" earth elements, may be approximated as follows:<sup>6</sup>

$$\vec{a} = \sum_{j=1}^N d\vec{a}_j, \quad (20)$$

where

$$d\vec{a}_j = K \left[ (\tau a E_s \cos \theta_s + e M_B) \frac{A_c}{mc \pi r^2} \cos \alpha dA \hat{r} \right]_j, \quad (21)$$

and  $N$  = total number of earth elements,

$\tau$  = 0 if the center of element  $j$  is in darkness,  
= 1 if the center of element  $j$  is in daylight.

Note that the longwave flux continues to act on the satellite, even if the center of an earth element is in darkness.

It would appear that Equations (20) and (21) are not very general with regard to satellite properties. However, even for geometrically complex satellites of high reflectivity, it is likely that a major portion of the earth radiation influence can be described by the "black body" term alone ( $K = 1$ ). Recall that this force is always directed along the element-satellite line, and (except for cross sectional area) is independent of satellite configuration. Any earth radiation

pressure forces not acting along the element-satellite line are primarily due to reflection (many satellites emit nearly isotropically in the infrared) the effect of which is scaled by a factor,  $a_s$ , usually much less than unity. Thus, a reasonable approximation to the earth radiation pressure acceleration on a non-spherical satellite would be Equations (20) and (21), in which the cross sectional area varies with the direction from which it is viewed.

#### Implementation

In order to perform the summation in Equation (20) such that the result approximates an analytical integration of Equation (19), McCarthy and Martin divide the earth's effective cap into segments which have equal projected areas. The UTOPIA version expands on this concept by organizing the effective cap into segments which have equal projected, *attenuated* areas. The projected, attenuated area is defined as the element area  $dA$  multiplied by the cosine of the view angle and divided by  $\pi$  times the square of the element-satellite distance, i.e.:

$$A' = \frac{dA_j \cos \alpha_j}{\pi r_j^2} \quad (22)$$

where  $A'$  is the projected, attenuated area of  $dA_j$ . Thus, by defining a weighting factor which is the same for all earth elements, several mathematical operations are saved for each evaluation of Equation (21).

Each area  $dA_j$  corresponds to the surface area of a portion of a sphere with radius equal to the mean radius of the earth. These earth segments are organized as shown in Figure 1. A "central cap" is located at the subsatellite point, and is surrounded by an arbitrary number of rings, each of which is divided into segments. In the nominal version of UTOPIA, there are two such rings; the first ring has six elements, and the second has 12 elements. This results in a total of 19 elements, counting the central cap. Various tests of the model indicate that this is the minimum total number of elements which still provides sufficient detail in the orbital effects.

For most models of earth radiation it is difficult to test the validity of the method described above in approximating the exact analytical integration over the effective cap. However, in the important limiting case of constant albedo, constant emissivity, and uniform illumination (i.e. no dependence on the solar zenith angle), this method produces a total acceleration, as calculated by Equations (20) and (21), which is a close numerical approximation to that obtained through analytical integration of Equation (19).

#### The Earth Radiation Model

Satellite data indicate that the albedo and emissivity of the terrestrial sphere display strong variations in latitude, and somewhat weaker longitudinal dependencies.<sup>5</sup> In addition, it is likely that the earth's rotation tends to average out any long period orbital effects engendered by longitudinal variations in earth radiation. On the basis of these arguments, many investigators use albedo and emissivity models which are exclusively latitude dependent.<sup>4, 5, 8, 17</sup> Also, note that the

most efficient general analytical representation of the earth radiation is probably a spherical harmonic expansion similar to that used in defining the gravity potential of the earth. For these reasons, the nominal UTOPIA model uses a purely zonal representation of the geographical distribution of earth radiation. It should be noted, however, that provisions are made in UTOPIA for including sectorial and tesseral terms, if desired.

Analyses of earth radiation budgets made by Stephens and others suggest that the albedo and emissivity may be modeled adequately using zeroeth, first and second degree zonal harmonics only, where the first zonal coefficient is periodic with a period of 365.25 days.<sup>12</sup> The model appears to be good enough to simulate both the latitudinal variation in earth radiation and a small seasonally dependent hemispherical asymmetry.

In sum, the nominal albedo and emissivity models may be represented as follows:

$$a = a_0 + a_1 P_1(\sin\phi) + a_2 P_2(\sin\phi), \quad (23)$$

$$e = e_0 + e_1 P_1(\sin\phi) + e_2 P_2(\sin\phi), \quad (24)$$

$$\text{where } a_1 = c_0 + c_1 \cos(\omega(JD-t_0)) + c_2 \sin(\omega(JD-t_0)), \quad (25)$$

$$e_1 = k_0 + k_1 \cos(\omega(JD-t_0)) + k_2 \sin(\omega(JD-t_0)), \quad (26)$$

$$t_0 = \text{epoch of the periodic terms,}$$

$$\omega = 2\pi/365.25 \text{ days}^{-1}.$$

The albedo and emissivity parameters for this model are  $a_0, c_0, c_1, c_2, a_2, e_0, k_0, k_1, k_2, e_2$ . Note that the time dependent nature of the albedo and emissivity parameters is limited to purely seasonal effects.

## Orbital Effects of Diffuse Earth Radiation

### Values of the Earth Radiation Constants

In order to evaluate the effects of earth radiation pressure on the trajectories of LAGEOS and other satellites, various constants in the force model and the earth radiation model must be chosen. As mentioned earlier, this study uses 19 earth segments to subdivide the effective cap. The solar irradiance, divided by the speed of light is calculated as follows:<sup>16</sup>

$$\frac{E_s}{c} = \frac{4.5605(10^{-6})}{r_{\text{EARTH}}^2} \quad (\text{Joules m}^{-3}), \quad (27)$$

where  $r_{\text{EARTH}}$  is the sun-earth distance in astronomical units. The earth radiation parameter values are obtained from least squares fits of Stephens' seasonal averages.<sup>12</sup> Values used in this study are:

$$a_0 = 0.34 \quad a_1[c_0 = 0., c_1 = 0.10, c_2 = 0.] \quad a_2 = 0.29$$

$$e_0 = 0.68 \quad e_1[k_0 = 0., k_1 = -0.07, k_2 = 0.] \quad e_2 = -0.18.$$

(The epoch value  $t_0$  is December 22, 1981.)

The remaining values required in the earth radiation pressure calculations are all satellite specific. The reflective and emissive properties of the satellites herein considered are all reasonably well known from studies of the direct solar radiation pressure. For a given satellite, these properties, as manifested in the augmentation factor, are typically lumped under the misnomer of "satellite reflectivity", here designated  $\eta$ . Hence:

$$K = 1 + \eta_E,$$

where  $\eta_E = a_s R + b_s \xi$ , the "satellite reflectivity" for the earth radiation calculations. The nominal values of  $\eta_E$  chosen for this study are all equal to the solar satellite "reflectivities"  $\eta_R$ .

The satellites examined in this study include the geodetic satellites LAGEOS (launched by the National Aeronautics and Space Administration (NASA) in 1978), Starlette (Centre Nationale d'Etudes Spatiale (CNES), 1975), GEOS-1 (NASA, 1965), and AJISAI (National Space Development Agency of Japan, 1985). The following table indicates the nominal orbital parameters, area to mass ratios, and earth radiation augmentation factors for each of these satellites, listed in order of ascending altitude.

Table 1 Satellite Properties

	altitude [km.]	eccentricity	inclination [deg.]	$A_0/m$ [m <sup>2</sup> Kg. <sup>-1</sup> ]	$\eta_E$
Starlette	953.	.02	49.8	.001	.12
AJISAI	1492.	.0006	50.1	.005	.15
GEOS-1	1690.*	.07	59.4	.007	.29
LAGEOS	5893.	.004	109.7	.0007	.13

\* perigee altitude = 1101 km., apogee = 2278 km.

## Character of Diffuse Earth Radiation Accelerations

### Variation with altitude

At first glance, it might appear that earth radiation pressure would obey a strict inverse square dependency on altitude, as suggested by Equation (21). It should be remembered, however, that the force exerted on a satellite due to earth emanations is the aggregate effect of all "active" earth segments, i.e. those earth elements in direct line-of-sight to the satellite. As the altitude increases, this "visible cap" increases thus compensating in some measure for inverse square attenuation. The cosine terms in (21), which are associated with illumination levels and viewing angles, vary both with altitude and position on the visible cap, thus further complicating the picture. It would seem, in any case, that the magnitude of this force should fall off according to a power law somewhat less severe than  $r^{-2}$ .

In this regard, consider a generalized, spherical satellite possessing an area-to-mass ratio of 0.01, and a reflectivity of 0.1. For the purposes of illustration, this satellite is placed directly over the subsolar point, and the total earth radiation pressure magnitude is calculated for altitudes between 200 km. and 6000 km. The solar radiation pressure and the drag force at these altitudes are also determined. The results are shown in Figure 3.

Figure 3 is a semilog plot of drag, solar radiation pressure, and earth radiation pressure acceleration magnitudes versus altitude. As expected, the magnitude of the solar radiation pressure is invariant with altitude, and the drag displays a characteristic exponential dropoff. Drag predominates over radiation pressure, both direct and reflected, at altitudes below 400 km., while radiation pressure

from both sources easily surpasses drag above 800 km. In the neighborhood of 600 km., all three forces share the same order of magnitude, but it is important to keep in mind the very considerable difference in the characteristic directions of each of these forces. As will be demonstrated later in this section, the earth radiation vector is largely radial; drag is primarily tangential, and solar radiation pressure acts along the sun-satellite line.

Above 400 km., the change in earth radiation pressure with altitude might best be described as a very gradual exponential decay. As expected, this represents a much more gradual decline than inverse square attenuation. Indiscriminate use of the inverse square law to extrapolate earth radiation values to higher altitudes could easily cause an underestimation of this force of several orders of magnitude.

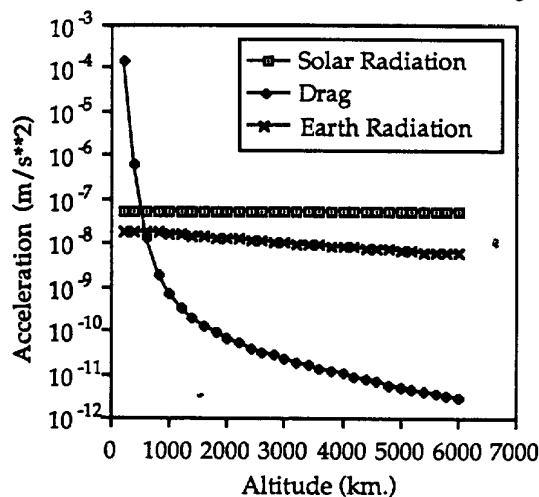


Fig. 3 Variation of Earth Radiation Pressure with Altitude ( $A_c/m = 0.01$ ,  $\eta_E = 0.1$ )

The unusual dependence of earth radiation pressure on altitude indicates that this force might be separable from gravity forces and other effects, given a data set consisting of high accuracy range observations of many satellites at various altitudes, or through observations of a single highly eccentric satellite.

#### Variation over an orbit

Due to the considerable changes in illumination as the satellite progresses in its orbit, the earth radiation pressure acceleration undergoes large variations in both direction and magnitude. For the purposes of this study, it is useful to follow a particular satellite, in this case LAGEOS, as it traverses a single revolution about the earth.

Figure 4 breaks the total earth radiation acceleration experienced during an eclipsing orbit into components in the radial, transverse, and normal directions. Note the predominance of the radial component, and the antisymmetric nature of the transverse component. Note also that the magnitude of the largest positive transverse acceleration is approximately equal to that of the greatest negative transverse acceleration. Given the assumption of diffuse terrestrial reflection and the nearly constant altitude of the satellite, the only variations in this quantity must arise solely from latitudinal variations in the earth radiation parameters. The maximum magnitude of the earth radiation acceleration is on

the order of  $10^{-10}$  m. sec.<sup>-2</sup>, which is about ten percent of the solar radiation acceleration on LAGEOS. This is in agreement with the results summarized in Figure 3.

The shortwave portion of the earth radiation acceleration undergoes significant variations over a single orbit. The longwave component is much less variable. In fact, the signature of the total earth radiation acceleration (magnitude) is essentially the same as that of the shortwave portion alone, biased by a nearly constant, primarily radial, longwave term. It would seem, therefore, that the influence of the longwave emitted radiation would be almost indistinguishable from a very small change in the gravitational constant of the earth, for low eccentricity orbits. (The adjustment in the earth's gravitational constant due to longwave earth radiation is approximately  $3(10^{-5})$  km<sup>3</sup> sec<sup>-2</sup>, which is two orders of magnitude smaller than the current uncertainty in the gravity parameter.) As a consequence, one would expect the shortwave component to have a greater orbital effect than the longwave component, in spite of the comparable magnitudes of their accelerations.

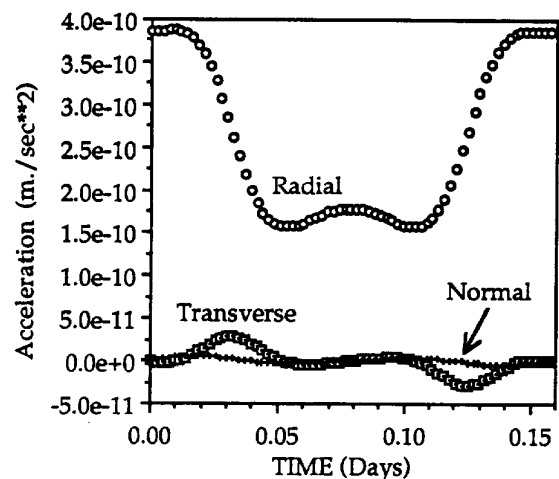


Fig. 4 Radial, Transverse, and Normal Earth Radiation Accelerations on LAGEOS

#### Earth Radiation Pressure and High Eccentricity Orbits

Satellites possessing highly eccentric orbits are of particular interest in the study of earth radiation pressure, due to the large variations in altitude experienced in the course of their orbits. In addition, in this class of satellite, the along-track acceleration is significantly affected by the projection of the very large radial acceleration component in the tangential direction. GEOS-1 has the largest eccentricity of the satellites cited in Table 1, and is examined in some detail.

In the case of high eccentricity orbits, it is instructive to examine the substantial difference between the tangential acceleration and the transverse acceleration. Figure 5 illustrates the discrepancy between these two components during a single orbit of GEOS-1, during which the satellite experiences deep eclipse. For this orbit, the average along track acceleration due to all earth radiation pressure is  $7.6(10^{-11})$  m s<sup>-2</sup>, as compared to the average transverse acceleration of  $5.5(10^{-12})$  m s<sup>-2</sup>. The average tangential acceleration is more than an order of magnitude larger than

the transverse because of the projection of the sizeable radial acceleration in the along-track direction. The average force over an orbit is nonzero because the eclipse causes an imbalance in the accelerations. As the maximum drag on this satellite is only  $(10^{-11}) \text{ m s}^{-2}$ , it is clear that the along track component of earth radiation pressure *during eclipse* tends to supercede the drag force in importance. During noneclipse orbits, the average tangential acceleration is much smaller, and somewhat more commensurate with the transverse acceleration. Note also that the magnitude and direction of the average earth radiation tangential acceleration depends on the exact nature of the eclipse event (e.g. a North-South eclipse versus a South-North eclipse passage), and the perigee location.

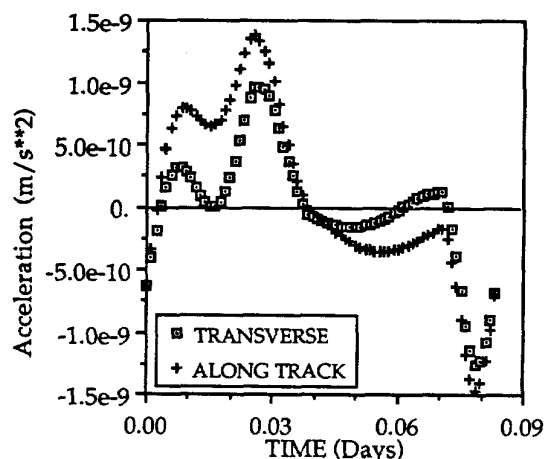


Fig. 5 Transverse and Along Track Earth Radiation Acceleration on GEOS-1 for an Eclipsing Orbit

#### Orbital Effects of Diffuse Earth Radiation

##### *A Comparison of Shortwave and Longwave Radiation Effects*

In order to determine the orbital influences of the various earth radiation components on LAGEOS and other satellites, the trajectory comparison option in UTOPIA has been used. A typical comparison run begins with the generation of a reference trajectory calculated with a given force model. A comparison trajectory obtained with a different force model is also generated. The reference trajectory is treated as a set of perfect observations for the comparison orbit, which is fit to the reference orbit in a least squares sense. The only parameters estimated in this portion of the study are the initial conditions (position and velocity). The number in the "total effect" column of the following table represents the RMS of the radial differences between a reference trajectory generated with the earth radiation pressure "turned on" and a comparison trajectory with earth radiation ignored. The result is an estimate of the "cost" in radial orbit error of ignoring earth radiation pressure, after the removal of all effects which are removable via estimation of the initial conditions.

The table below displays the significant difference between the orbital effects of earth's shortwave and longwave

radiation. For three different satellites the evidence is clear that the longwave emitted component by itself accounts for only ten percent or so of the total orbital influence of earth radiation. The broadband shortwave (reflected) flux of the earth accounts for almost all of the earth radiation effects.

Table 2 Comparison of Shortwave and Longwave Effects

	arc [days]	Shortwave Radial diff. [meters]	Longwave Radial diff. [meters]	Total Effect Radial diff. [meters]
Starlette	30.	.10	.008	.11
LAGEOS	365.	.40	.026	.42

##### *Diffuse Earth Radiation and the Secular Decrease in the Semimajor Axis of LAGEOS*

Figure 6 plots the changes in semimajor axis for LAGEOS during a 365 day arc in which a nominal trajectory is generated with earth radiation pressure activated, and a comparison trajectory is generated with earth radiation pressure absent from the force model. The comparison trajectory is fitted to the nominal orbit via the estimation of initial conditions and solar radiation reflectivity. If earth radiation pressure were the sole cause of LAGEOS' anomalous behavior, then the plot would reveal a linear trend, with a maximum deviation of 0.4 meter at the end of the arc. It is clear instead that the envelope of the semimajor axis residuals undergoes a *periodic* fluctuation with a mean near zero, no significant secular trend, and a maximum excursion of 0.03 meter. Frequency analyses of somewhat longer arcs reveal significant periodicities at multiples of 280 days, which is half the period of one revolution of LAGEOS' node with respect to the sun. It is evident that the mysterious behavior of LAGEOS is not explicable in terms of diffuse earth radiation pressure.

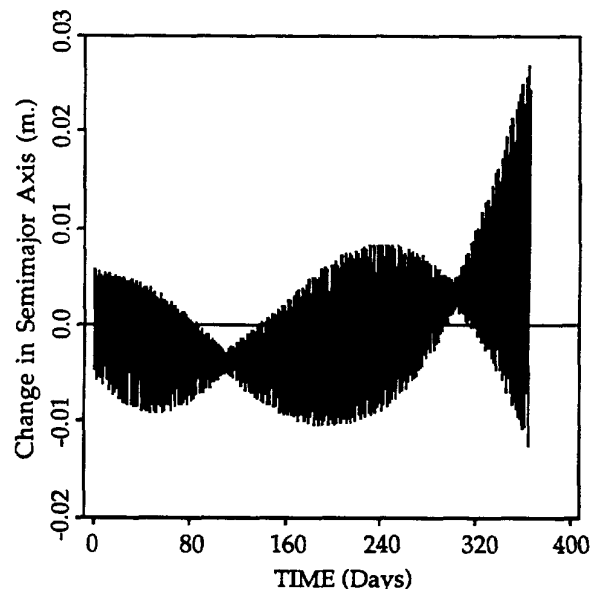


Fig. 6 Change in Semimajor Axis of LAGEOS due to Earth Radiation Pressure



With the exception of the longitude of the ascending node, shown in Figure 7, all other orbit elements show only small, long period fluctuations due to earth radiation pressure. The node's perturbation shows a secular rate of  $1.3(10^{-3})$  arcseconds per year. This is somewhat higher than the prediction of  $0.6(10^{-3})$  arcsecond per year made by Rubincam and Weiss.<sup>8</sup> The difference is likely due to the inclusion of longwave earth radiation pressure in the UTOPIA model.

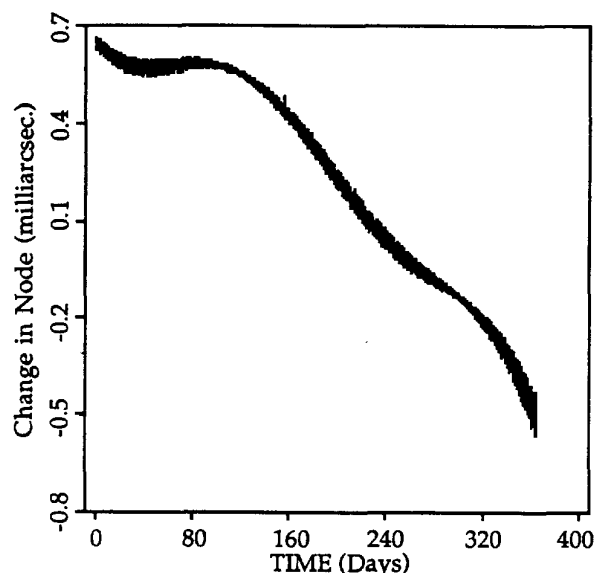


Fig. 7 Change in Longitude of Ascending Node of LAGEOS due to Earth Radiation Pressure

#### Earth Radiation Effects on other Satellites

The following table shows the orbital effects of earth radiation on the satellites described in Table 1. "Percent shadow" refers to the percentage of time the given satellite is in earth shadow, and is intended to give some indication of the lighting conditions during the arc. Just as before, the orbital effects are quantified using a trajectory comparison run in which the nominal trajectory has earth radiation activated and the comparison orbit has earth radiation turned off.

Table 3 Diffuse Earth Radiation Effects

	arc [D.]	Estimated Parameters	Percent Shadow	Radial RMS[m.]	Transverse RMS[m.]
Starlette	30.	IC	32.	.11	4.03
	30.	IC, $C_D$ , $\eta_R$	32.	.01	.15
AJISAI	30.	IC	15.	.35	.70
	30.	IC, $C_D$ , $\eta_R$	15.	.03	.08
GEOS-1	30.	IC	10.	1.8	34.2
	30.	IC, $C_D$ , $\eta_R$	10.	1.4	3.7
LAGEOS 365.	365.	IC	7.	.42	8.4
	365.	IC, $C_T^*$ , $\eta_R$	7.	.42	3.96

\* $C_T$ : along track drag coefficient.

Note the disproportionately large RMS values for GEOS-1, which, with an eccentricity of 0.07, has the most eccentric orbit. This lends support to the theory that high eccentricity satellites tend to exhibit a particularly high degree of sensitivity to earth radiation pressure. It might be argued that Starlette should demonstrate some of the same sensitivity, in view of its lower altitude and orbital eccentricity of 0.02. Recall, however, that Starlette's area to mass ratio is seven times smaller than that of GEOS-1. Also, the difference between Starlette's perigee and apogee heights is only about 300 km., while the altitude of GEOS-1 varies by almost 1200 km. over an orbit. An analysis of GEOS-1 data is included in the following section.

#### The Effects of Diffuse Earth Radiation Pressure on GEOS-1

Recent analyses of GEOS-1 tracking data suggest the presence of unmodelled forces on the satellite. Specifically, the best available data fits include long intervals during which drag coefficient estimates are large and negative, indicating the presence of positive along track accelerations of the same order as drag. The largest negative drag coefficients occur during a period of eclipse, but the negative  $C_D$  values do not appear to be confined to shadowing events. The interval possessing the largest measures of negative drag includes the deep eclipse orbit of Figure 5. The nonconservative tangential accelerations on GEOS-1, averaged over this orbit, are indicated in the following table, where "positive" is in the direction of motion.

Table 4 Average Tangential Accelerations on GEOS-1 due to Nonconservative Forces

eclipsing orbit (6-27-77)	
SOLAR RAD. PRESSURE	$1.7 \text{ E-9 m s}^{-2}$ (positive)
ATMOS. DRAG ( $C_D = 3.0$ )	$1.3 \text{ E-10 m s}^{-2}$ (negative)
EARTH RAD. PRESSURE	$8.2 \text{ E-11 m s}^{-2}$ (positive)

It is evident that the dominant nonconservative along track acceleration on the satellite in this orbital orientation is the solar radiation pressure. Note, however, that the tangential component of earth radiation pressure, averaged over this eclipsing orbit, is of the same order as drag, and is in the positive along track direction as well. It is clear that errors in the determination of either solar radiation pressure or earth radiation pressure may be capable of generating the observed negative  $C_D$  values.

One possible source of error in the determination of solar radiation pressure involves variations in the area which intercepts the solar flux. GEOS-1 is a gravity-gradient stabilized satellite, which presents the same surface to the earth at all times, and thus presents a continually varying cross section to the sun. In addition, the earth pointing "bottom" of the satellite is highly reflective, while the "sides" are covered by dark solar cells. An extreme case, in which the side area is assumed to be 1/10th as reflective as the underside, leads to only a small "improvement" in the  $C_D$  values, in the sense that they are made slightly less negative. Various other area variations have been tested, without significantly affecting the  $C_D$  levels.

As mentioned earlier, the earth radiation pressure on this satellite is also capable of generating sizeable along track accelerations. Analyses indicate that estimating the zeroeth degree albedo parameter  $a_0$  produces a highly salutary effect on the "worst" drag coefficients. In fact, among the various estimated parameters examined in this study, only albedo has a dramatic effect on the extremely large negative  $C_D$  values present in the arc starting 6-27-77. Some further improvement is effected when a variable area solar radiation pressure model is added.

Figure 8 illustrates the influence of earth radiation pressure on drag coefficients estimated during a 30 day arc starting June 27, 1977. At the start of the arc, the orbit of the satellite passes through deep shadow. As the arc progresses, nodal precession causes the orbit to move entirely out of shadow by July 11 (day 14 on the plot). One drag coefficient is estimated for each 3 day interval in the arc. Nominally, a single solar radiation reflectivity is estimated for the entire 30 day trajectory. The largest negative drag coefficients occur when earth radiation pressure is ignored completely, as depicted by the bottom line in Figure 8. When the nominal earth radiation model is utilized, there is a measurable improvement in the  $C_D$  values, in the sense that they are driven towards a more physically reasonable level. Some additional improvement is evident when, in addition, solar radiation reflectivities are estimated every 5 days. This run is characterized by reasonable values of solar reflectivity in the early, eclipsing part of the arc, followed by physically impossible (i.e. negative) values outside this region. As Figure 8 indicates, this case also exhibits equally unlikely large positive  $C_D$  estimates towards the end of the arc.

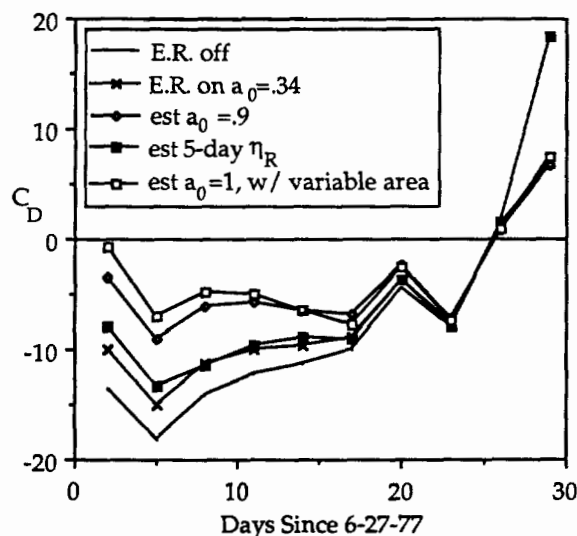


Fig. 8 Effects of Earth Radiation Pressure on GEOS-1 drag Coefficients

The most dramatic improvements in the  $C_D$  values occur when the zeroeth degree albedo parameter is estimated. The two uppermost lines on Figure 8 show the effects of estimating  $a_0$  on the drag coefficients, with and without the benefit of a 30% solar pressure area variation model. In regions of deep eclipse, estimation of  $a_0$  results in  $C_D$  values which are one tenth to one half the size of those estimated

without the benefit of earth radiation pressure. The estimated values of  $a_0$  are extremely high, however, approaching unity in both cases.

The impact of earth radiation pressure decreases smoothly as the satellite's orbit moves away from the eclipse region. Even when the satellite no longer enters the shadow itself, the average earth radiation pressure over an orbit is influenced by the unlit hemisphere. By the time the orbit is well out of shadow, however, the earth radiation imbalance which caused a significant along track acceleration has disappeared. Thus the latter portion of the arc depicted in Figure 8 shows drag coefficients insensitive to earth radiation pressure.

The motion of the satellite during the arc described above is such that eclipse is traversed from South to North. When the node has precessed sufficiently, the eclipse passage is North to South, and the sense of the average tangential earth radiation acceleration is reversed. In this case, the earth radiation pressure engenders a net deceleration, which might conceivably cause the  $C_D$  values to become even more negative to compensate. A 30 day orbit fit characterized by a North to South eclipse results in very small improvements in the drag coefficients. The significant result in this case is that, while the  $C_D$ 's are not markedly "improved", neither are they made any poorer.

The exact origins of the large negative  $C_D$ 's for GEOS-1 are still not clear. As Figure 8 indicates, even when an unusually high albedo value is used, many  $C_D$  estimates remain at an uncomfortably large negative level. Also, despite the manifest impact of earth radiation pressure on the drag coefficients, the orbit fit is not improved by the estimation of albedo parameters. All this suggests that another, or perhaps several other unmodelled or mismodelled mechanisms are at work. Some mismodelling of the solar radiation pressure may still play a part in this, despite the relatively small effect on the  $C_D$ 's engendered by various solar pressure configurations. Keeping in mind that the problem is still unresolved, it is clear that earth radiation pressure can affect parameter estimation to a significant degree.

## Conclusions

Returning to the provenance of this study, it would appear that diffuse earth radiation is unable to explain the anomalous residual behavior of LAGEOS' semimajor axis. The along track force on this satellite due to diffuse earth emanations is simply too small and periodic to produce the observed secular trend in the semimajor axis. The total force does not appear to generate any significant portion of the observed periodic behavior in the semimajor axis. There is a small secular change apparent in the node.

In the broader sense, it is evident that the orbital effects of diffuse earth radiation pressure are small but not always negligible. When the eccentricity of the satellite's orbit is small, the greater portion of the influence of earth radiation may be absorbed in the estimation of standard parameters. High eccentricity satellites are particularly sensitive to earth radiation pressure, especially during periods of deep eclipse. During such events, sizeable along-track accelerations can develop which do not average out in the course of an orbit. This can have a significant impact on the

recovery of estimated parameters, including drag coefficients.

It has been demonstrated that the orbital perturbation due to longwave radiation amounts to only about ten percent of the total earth radiation pressure effect. Thus, any improvements in the earth radiation pressure model must be directed towards the shortwave component.

### Acknowledgements

Computations were carried out on a Cray X-MP/24 supercomputer at The University of Texas System, Center for High Performance Computing. This work was supported by NASA contract NAS-528192.

### References

<sup>1</sup>Anselmo, et al., "Effects of the Earth-Reflected sunlight on the Orbit of the LAGEOS satellite," *Astronomy and Astrophysics*, 117, 3-8, 1983.

<sup>2</sup>Barlier, et al. "Non-gravitational Perturbations on the Semimajor Axis of LAGEOS," *Annales Geophysicae*, 4, A, 3, pp. 193-210, 1986.

<sup>3</sup>Bernard, A., et al., "Radiation Pressure Determination With the Cactus Accelerometer," *COSPAR Space Research*, 1978.

<sup>4</sup>Lautmann, D. A., "Perturbations of a Close-Earth Satellite Due to Sunlight Diffusely Reflected from the Earth," *Celestial Mechanics*, 16, pp. 3-25, 1977.

<sup>5</sup>Lochry, Robert R., "The Perturbative Effects of Diffuse Radiations from the Earth and Moon on Close Satellites," Dept. of Engineering, UCLA, Ph.D. Dissertation, 1966.

<sup>6</sup>McCarthy, J. J., and Martin, T. V., "A Computer Efficient Model of Earth Albedo Satellite Effects," NASA Goddard Space Flight Center, Planetary Sciences Department Report no. 012-77, June 1977.

<sup>7</sup>Morgan, W. J., "Morning/Evening Difference in Earth's Albedo and the Deceleration of LAGEOS," *EOS*, 65, p. 855, 1984.

<sup>8</sup>Rubincam, David P., and Weiss, Nelson R., "Earth Albedo and the Orbit of LAGEOS," National Aeronautics and Space Administration, Technical Memorandum 86210, June, 1985.

<sup>9</sup>Rubincam, et al., "Earth Anisotropic Reflection and the Orbit of LAGEOS," *Journal of Geophysical Research*, 92, no. B11, pp. 11662-11668, October, 1987.

<sup>10</sup>Rubincam, David P., "Yarkovsky Thermal Drag on LAGEOS," manuscript submitted to *Journal of Geophysical Research*, 1988.

<sup>11</sup>Smith, D. E., and Dunn, P. J., "Long Term Evolution of the LAGEOS Orbit," *Geophysical Research Letters*, 7, pp. 437-440, 1980.

<sup>12</sup>Stephens, et al., "Earth Radiation Budgets," *Journal of Geophysical Research*, 86, no. C10, pp. 9739-9760, October, 1981.

<sup>13</sup>Suits, Gwynn H., "Chapter 3: The Nature of Electromagnetic Radiation," *Manual of Remote Sensing*, Vol. 1, Ed. Robert G. Reeves, American Society of Photogrammetry, Falls Church, Va., 1975.

<sup>14</sup>Taylor, V. R., and Stowe, L. L., "Reflectance Characteristics of Uniform Earth and Cloud Surfaces Derived from NIMBUS-7 ERB," *Journal of Geophysical Research*, 89, no. D4, pp. 4987-4996, June, 1984.

<sup>15</sup>Walch, J. J. translation of: "Choix d'un modele de rayonnement d'albedo terrestre. Calcul pratique de son effet sur la trajectoire d'un satellite," *The Use of Artificial Satellites for Geodesy and Geodynamics*, Vol. 3, edited by G. Veis, pp. 172-182, National Technical University, Athens, 1984.

<sup>16</sup>Willson, Richard C., "Accurate Solar 'Constant' Determinations by Cavity Pyroheliometers," *Journal of Geophysical Research*, 83, no. C8, p. 4003, August, 1978.

<sup>17</sup>Wyatt, Stanley P., "The Effect of Terrestrial Radiation Pressure on Satellite Orbits," *Dynamics of Satellites Symposium*, IUTAM, 28-30 May 1962, Paris, Ed. M. Roy, Academic Press, New York, 1963, pp. 180-196.